Engineering Nickel Catalysts with Atomic-Sulfur-Stabilized Thiolate Adlayers for Durable Selectivity in Hydrogenation of Halonitrobenzenes

Yujian Fan[a,†], Xuechun Sang[a,†], Juwen Gu[b,†], Songbai Qiu[a,c,d,*], Tiejun Wang[a,c,d,*]

[a] School of Chemical Engineering and Light Industry, Guangdong University of Technology, Guangzhou 510006, China.

[b] Key Laboratory of Guangdong Higher Education Institutions of Northeast Guangdong New Functional Materials, School of Chemistry and Environment, Jiaying University, Meizhou 514015, China.

[c] Guangdong Provincial Key Laboratory of Plant Resources Biorefinery, Guangzhou 510006, China.

[d] Guangzhou Key Laboratory of Clean Transportation Energy and Chemistry, Guangzhou 510006, China.

† These authors contributed equally to this work.

* To whom correspondence should be addressed. E-mail: qiusb@gdut.edu.cn (S. Q), tjwang@gdut.edu.cn (T. Wang)

1. EXPERIMENTAL SECTION

1.1. Materials

Nickel (II) nitrate hexahydrate ($Ni(NO_3)_2·6H_2O$, 98.0%) was purchased from Guangzhou Chemical Reagent Factory Co., Ltd., China. L-cysteine (99.7%), ethanol (EtOH, 99.7%), *o*-chloronitrobenzene (*o*-CNB, 99.9%), citric acid monohydrate (99.5%), tetraethyl orthosilicate (99.5%), various nitrobenzene compounds and thiols were obtained from Macklin Biochemical Co., Ltd., China. All the chemicals were used as received without further purification.

1.2. Catalyst Synthesis

1.2.1. Synthesis of Ni@C catalysts. The Ni@C catalysts were synthesized via a sol-gel method. Specifically, $Ni(NO_3)_2·6H_2O$ (23.7 mmol) and citric acid monohydrate (47.5 mmol) were dissolved in 100 mL of deionized water and stirred at 80 °C until complete dissolution. The mixture was gradually gelled by continuous heating and stirring, followed by oven drying at 95 °C. The dried gel was carbonized at 550 °C for 2 h under a N_2 atmosphere with a heating rate of 5 °C·min^{-1} to obtain the Ni@C catalysts.

1.2.2. Synthesis of Ni@C-SH-*x*-*y* catalysts. The as-synthesized Ni@C catalyst was first reduced under a hydrogen atmosphere at 400 °C for 1 h prior to the modification process. Typically, 0.3 g of Ni@C, 16.5 mmol of *n*-octanethiol, and 40 mL of EtOH were added into a 100 mL Teflon-lined autoclave. The mixture was heated at 120 °C for 12 h. The resulting product was separated by centrifugation, washed thoroughly with EtOH and dried overnight. The as-synthesized material was designated Ni@C-SH-120-12. For a systematic study, a series of Ni@C-SH-*x*-*y* catalysts were synthesized under identical conditions, employing modified reaction temperatures (x = 25–180 °C) and durations (y = 3–24 h).

1.2.3. Synthesis of Ni@C-S_z catalysts. The Ni@C-S_z catalysts were prepared according to literature [1]. $Ni(NO_3)_2·6H_2O$ (23.7 mmol), citric acid monohydrate (47.5 mmol) and L-cysteine

(0.79/0.948/4.86 mmol) were dissolved in 100 mL of deionized water and stirred at 80 °C until complete dissolution. The mixture was gradually gelled by continuous heating and stirring, followed by oven drying at 95 °C. The dried gel was carbonized at 550 °C for 2 h under a N_2 atmosphere with a heating rate of 5 °C·min^{-1} to obtain the Ni@C-S_z catalyst, where *z* represents the molar ratio of Ni/S.

1.2.4. Synthesis of Ni/SiO_2 catalyst. The Ni/SiO_2 catalyst was prepared via a sol–gel method. Typically, $Ni(NO_3)_2 \cdot 6H_2O$ (17.0 mmol) and citric acid monohydrate (17.0 mmol) were dissolved in 50 mL of deionized water. After complete dissolution, tetraethyl orthosilicate (83.2 mmol) was added, and the mixture was stirred at room temperature until homogeneous. The solution was then heated to 70 °C under continuous stirring to form a uniform gel. The resulting gel was dried at 90 °C to obtain a xerogel. The dried product was calcined in air at 500 °C for 2 h to yield NiO/SiO_2. For each catalytic test or modification experiment, 0.1 g of the as-prepared NiO/SiO_2 was first reduced in a H_2 flow at 500 °C for 2 h to obtain metallic Ni/SiO_2, which was then immediately protected with EtOH to prevent oxidation.

1.2.5. Synthesis of Ni/SiO_2-SH-120-3 catalyst. The thiolate-modified catalyst was prepared following a similar procedure to that described for Ni@C-SH-*x*-*y*. Typically, 0.1 g of NiO/SiO_2 was first reduced in H_2 at 500 °C for 2 h. The freshly reduced Ni/SiO_2 was then transferred into a 50 mL Teflon-lined autoclave containing *n*-octanethiol (1.4 mmol) and EtOH (10 mL). The mixture was heated at 120 °C for 3 h. After cooling to room temperature, the resulting solid was separated by centrifugation, washed thoroughly with EtOH, and dried overnight. The obtained catalyst is denoted as Ni/SiO_2-SH-120-3.

1.3. Catalyst Characterization

X-ray diffraction (XRD) patterns were obtained using a Rigaku Mini Flex 600 diffractometer with Cu Kα radiation (λ = 0.15406 nm), scanning over a 2θ range from 10° to 80°. The textural properties and morphologies of catalysts were characterized by scanning electron microscopy (SEM, Hitachi SU8010). Energy-dispersive X-ray spectroscopy (EDS) elemental mapping was performed using Talos F200X and Themis Z instruments. The nickel content of the catalysts was determined by inductively coupled plasma optical emission spectrometry (ICP-OES) using a Thermo Fisher iCAP 7400 analyzer. Sulfur and carbon contents in the catalysts were determined on a Vario El cube elemental analyzer.

Density Functional Theory (DFT) calculations: All DFT calculations were carried out using the Vienna Ab initio Simulation Package (VASP). The exchange-correlation functional employed was the Perdew-Burke-Ernzerhof (PBE) functional within the generalized gradient approximation (GGA). To calculate adsorption energies, the DFT-D method was used to account for van der Waals interactions between adsorbates, with a vacuum layer thickness set to 15 Å. The valence electrons were described by a plane-wave basis set with a kinetic energy cutoff of 400 eV, and the core electrons were replaced by the projector augmented wave (PAW) pseudopotentials. The k-points were set to 2×2×1. A three-layer slab model with a 3×3 supercell was constructed, with the top layer allowed to relax. All structures were optimized until the forces on each atom were less than 0.01 eV/Å.

1.4. Catalyst Testing

The hydrogenation of *o*-CNB was carried out in a 50 mL stainless steel autoclave reactor equipped with a magnetic stirrer. Typically, 0.5 g *o*-CNB, 0.1 g catalyst, and 10.0 g EtOH (reaction solvent) were loaded into the reactor. The reactor was flushed with H_2 more than three times to

remove the air, and subsequently pressurized to 2 MPa with H_2. Reactions proceeded at predetermined temperatures with magnetic stirring (1000 rpm) for specified durations.

For the in-situ modification experiment, thiol was directly added to the reaction solution for in situ modifying Ni@C catalyst during the reaction.

Upon completion, the reactor was cooled to room temperature and H_2 stream was vented to atmospheric pressure. Reaction products were qualitatively identified using an Agilent 8890 gas chromatograph (GC) coupled with a 5977C mass-selective detector (MSD). Helium carrier gas flowed at 0.48 $mL \cdot min^{-1}$, with separation achieved on an HP-5MS capillary column (30 m × 250 μm × 0.25 μm). The GC oven temperature program initiated at 40 °C (held for 5 min), ramped to 180 °C at 5 $°C \cdot min^{-1}$, then to 320 °C at 15 $°C \cdot min^{-1}$ (held for 5 min). The MSD was operated in selected ion monitoring (SIM) mode with electron impact ionization. Reaction products were quantified using a Shimadzu 2010 Pro gas chromatograph (GC) with separation achieved on a WondaCap 5 column (30 m × 530 μm × 1.5 μm). The oven temperature program for the Shimadzu 2010 Pro gas chromatograph was set as follows: initiated at 50 °C (held for 1 min), ramped to 220 °C at 10 $°C \cdot min^{-1}$ (held for 1 min). Conversion of *o*-CNB and selectivity of *o*-CAN were calculated as follows:

$$\text{Conversion}\ (\%) = \left(1 - \frac{\text{Moles of feedstock after the reaction}}{\text{Moles of feedstock before the reaction}}\right) \times 100\%$$

$$\text{Selectivity}\ (\%) = \frac{\text{Moles of target product}}{\text{Moles of all products}} \times 100\%$$

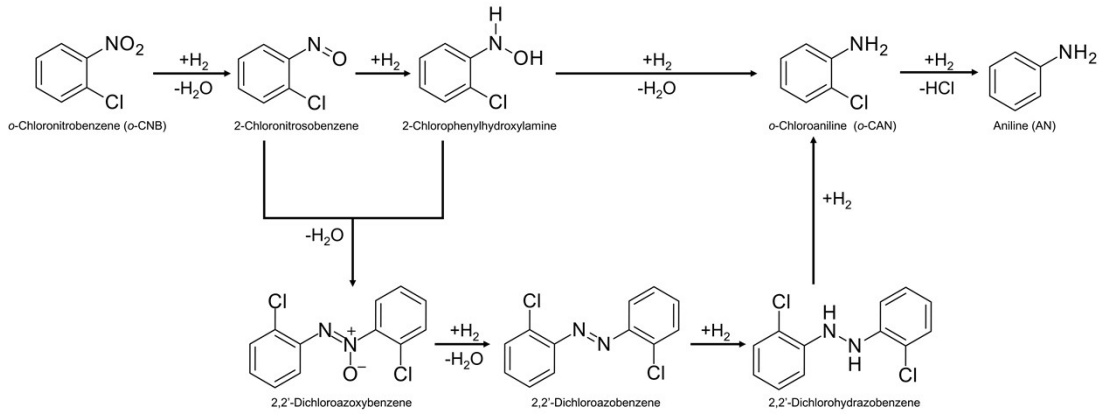

Fig. S1 The proposed mechanism of *o*-CNB hydrogenation.

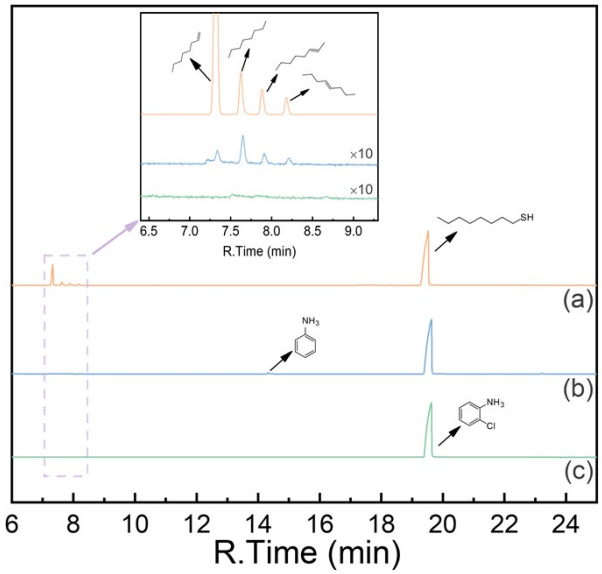

Fig. S2 (a) GC-MS profiles of the liquid products obtained from the post-modification solution, (b, c) GC-MS profiles of the liquid products obtained from the catalytic reaction over the resulting catalysts: (b) Ni@C-SH-120-3 and (c) Ni@C-SH-120-12. Modification conditions: 0.3 g Ni@C catalyst, 40 mL EtOH, 16.5 mmol *n*-octanethiol, 120 °C, 12 h. Reaction conditions: 0.5 g *o*-CNB, 0.1 g catalyst, 10.0 g EtOH, 2 MPa H_2, 80 °C, 2 h.

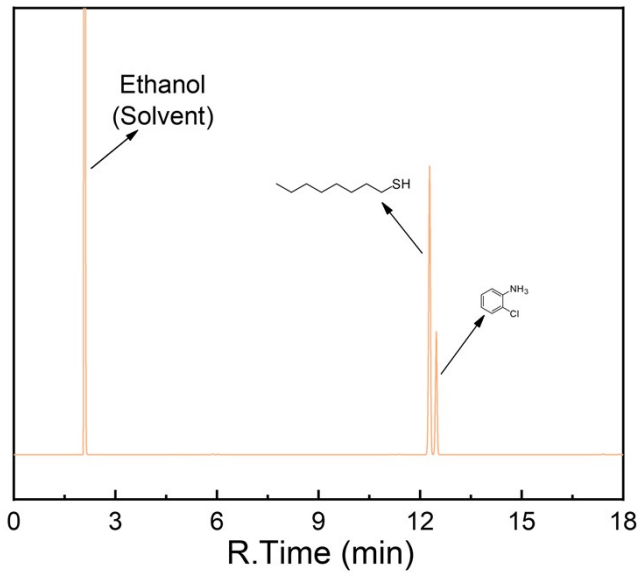

Fig. S3 GC profiles of the reaction products obtained from in-situ modification experiment over the unmodified Ni@C catalyst. Reaction conditions: 0.5 g *o*-CNB, 0.1 g catalyst, 10.0 g EtOH, 5.5 mmol *n*-octanethiol, 2 MPa H_2, 100 °C, 8 h.

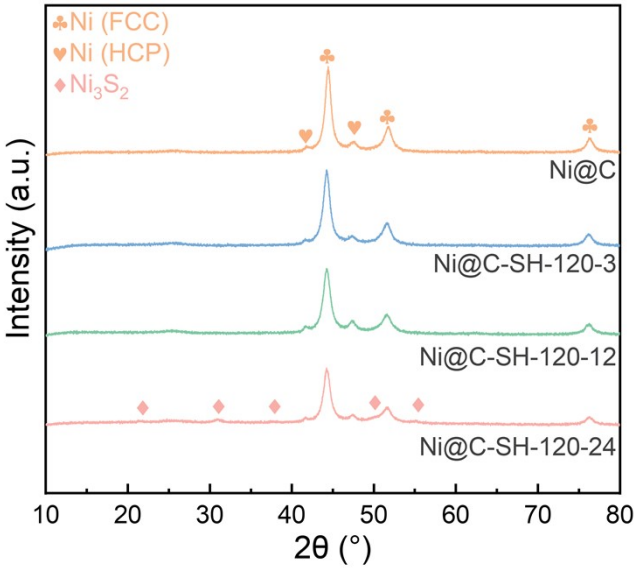

Fig. S4 XRD patterns of the Ni@C-SH-120-*y* catalysts synthesized at different modification times.

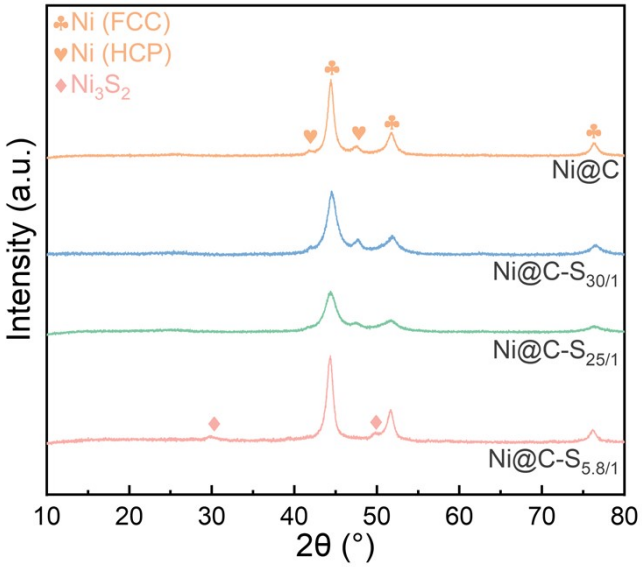

Fig. S5 XRD patterns of the Ni@C-S_z catalysts synthesized with different sulfur contents.

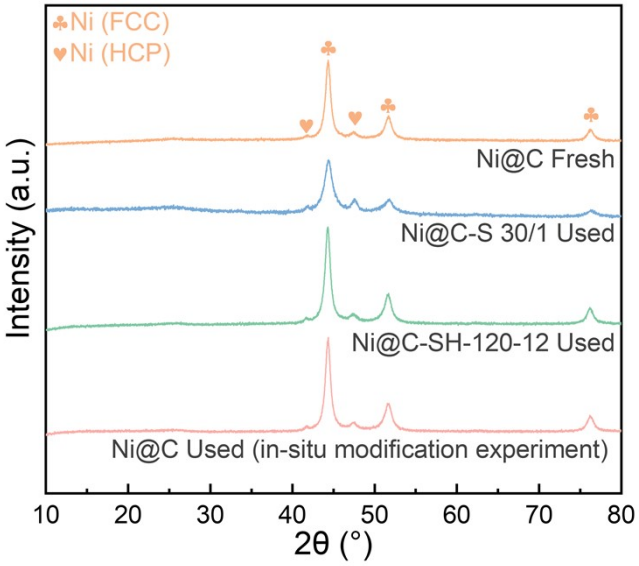

Fig. S6 XRD patterns of the catalysts after the reaction.

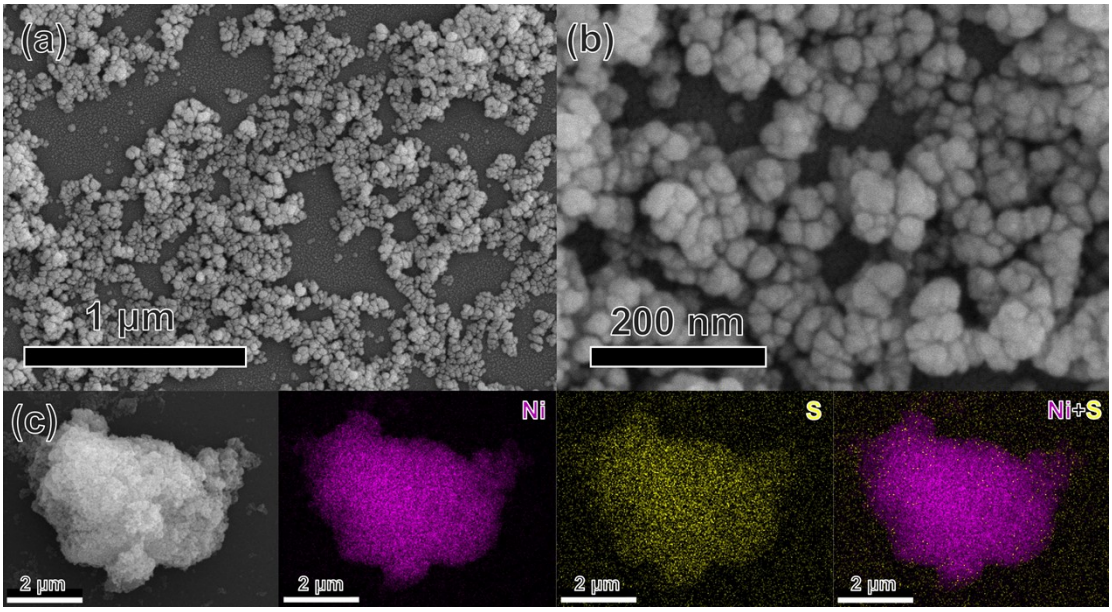

Fig. S7 SEM image and EDS elemental mappings of Ni@C-SH-120-12 catalyst.

Table S1. Elemental composition of the Ni@C-SH-120-12 catalyst.

Atomic (%)	ICP-OES/ elemental analysis[a]	XPS
C	31.6	80.3
S	3.4	2.7
Ni	15.5	9.9
Ni:S	**4.6**	**3.7**

[a] S and C contents in the catalysts were determined by elemental analysis. Ni contents in the catalysts were determined by ICP-OES analysis.

The nickel-to-sulfur (Ni:S) atomic ratio was determined to be 3.7 by XPS and 4.6 by ICP-OES/elemental analysis. As XPS is a surface-sensitive technique while ICP-OES/elemental analysis probes the bulk composition, the low Ni:S ratio from XPS indicates an enrichment of sulfur species on the catalyst surface [2].

Table S2. The relative contents and binding energies of S species in the samples [a].

Catalysts	Content (at%)		
	Ni-S atomic sulfur (161.9 eV)	C-S adsorbed thiolates (162.6 eV)	C-S free thiols (163.1 eV)
Ni@C-SH-120-3	12%	49%	40%
Ni@C-SH-120-12	19%	50%	31%
Ni@C-SH-160-3	38%	37%	24%

[a] Calculated from XPS spectra of S $2p_{3/2}$ regions.

Table S2 clearly show that as the modification temperature and time increase, the content of free thiol (C–S, 163.1 eV) decreases, while the concentrations of adsorbed thiolates (C–S, 162.6 eV) and atomic sulfur in a Ni–S configuration (161.9 eV) increase sequentially. This trend provides direct quantitative evidence for the stepwise cleavage of S–H and C–S bonds during the thermal-induced modification process.

Table S3. The relative contents and binding energies of Ni species in the samples [a].

Catalysts	Content (at%)		
	Ni^0 (853.0 eV)	NiO (853.8 eV)	Ni^{2+} (856.1 eV)
Ni@C	54%	22%	24%
Ni@C-SH-120-3	55%	20%	26%
Ni@C-SH-120-12	48%	23%	29%
Ni@C-SH-160-3	27%	17%	56%

[a] Calculated from XPS spectra of Ni $2p_{3/2}$ regions.

Table S3 summarizes the corresponding changes in nickel species. The increase in the proportion of Ni^{2+} species (856.1 eV) correlates directly with the rising atomic sulfur content, reflecting electron transfer from Ni to S. This charge transfer is the electronic origin of the observed downshift in the Ni d-band center and is concomitant with the formation of nickel sulfide phases at elevated modification temperatures, as discussed in Section 3.1.

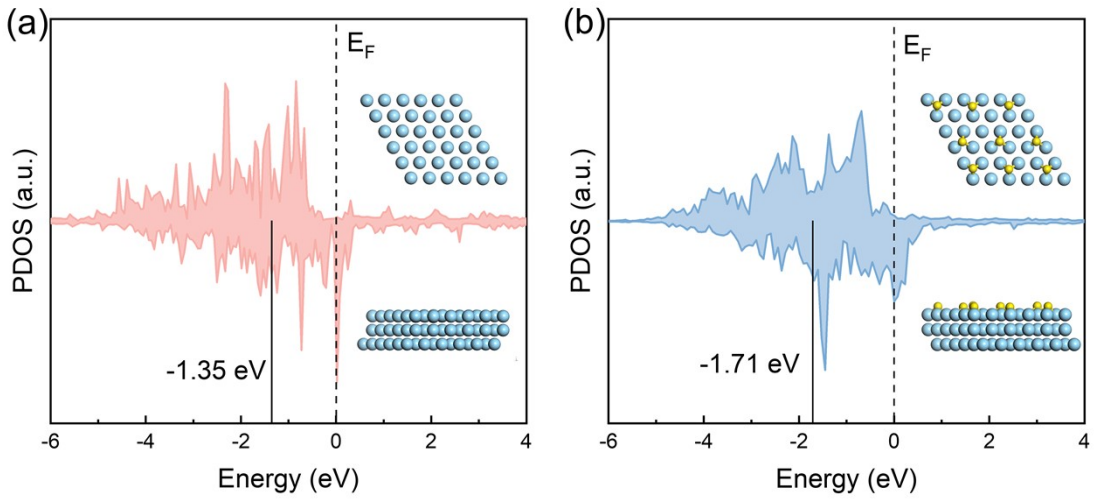

Fig. S8 PDOS of Ni_{3d} orbitals for (a) clean Ni (111) and (b) Atomic-sulfur-modified Ni (111).

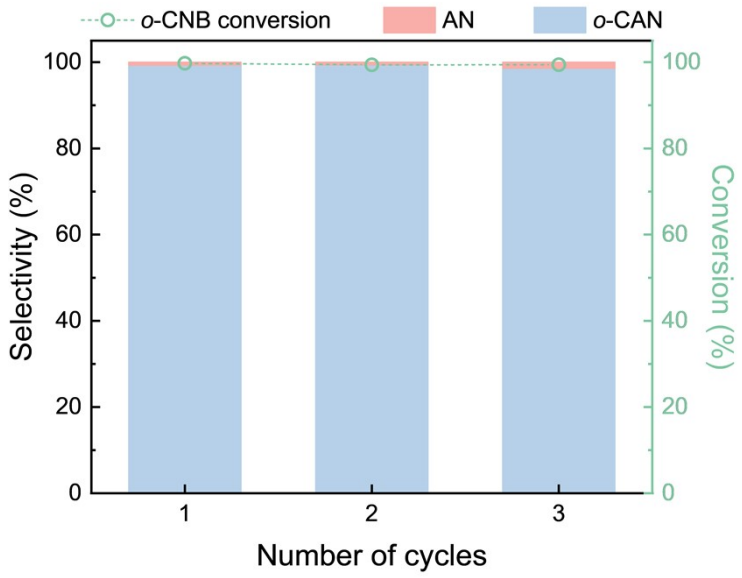

Fig. S9 Recycling stability of Ni@C-SH-120-3. Reaction conditions: 0.5 g *o*-CNB, 0.1 g catalyst, 10.0 g EtOH, 2 MPa H_2, 80 °C, 2 h.

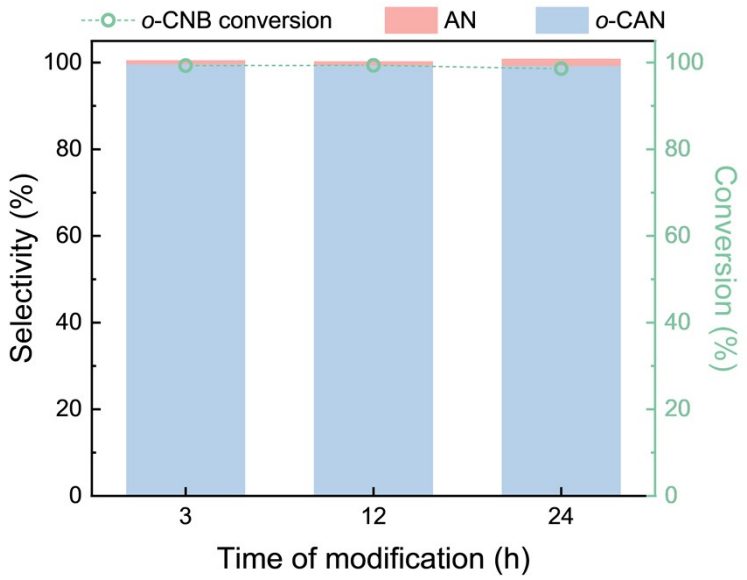

Fig. S10 *o*-CNB conversion and *o*-CAN selectivity over Ni@C-SH-120-*y* catalysts synthesized at different modification times. Reaction conditions: 0.5 g *o*-CNB, 0.1 g catalyst, 10.0 g EtOH, 2 MPa H_2, 100 °C, 8 h.

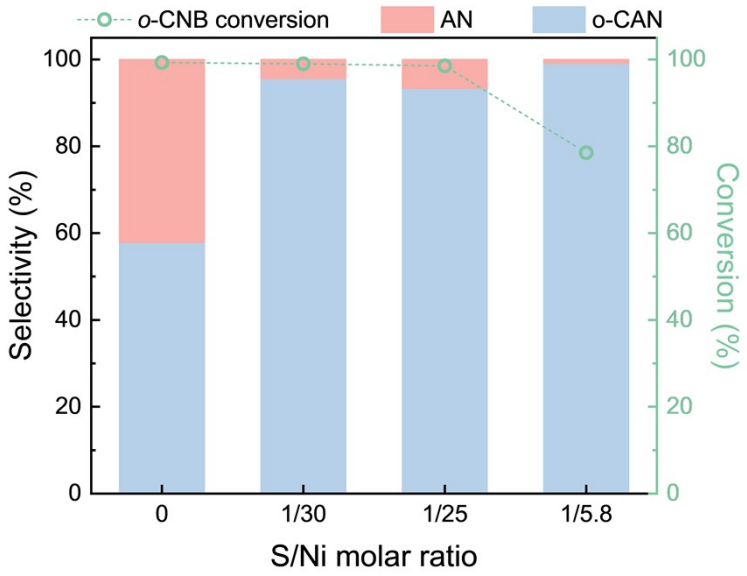

Fig. S11 *o*-CNB conversion and *o*-CAN selectivity over Ni@C-S_z catalysts prepared with different S/Ni mass ratios. Reaction conditions: 0.5 g *o*-CNB, 0.1 g catalyst, 10.0 g EtOH, 2 MPa H_2, 100 °C, 8 h.

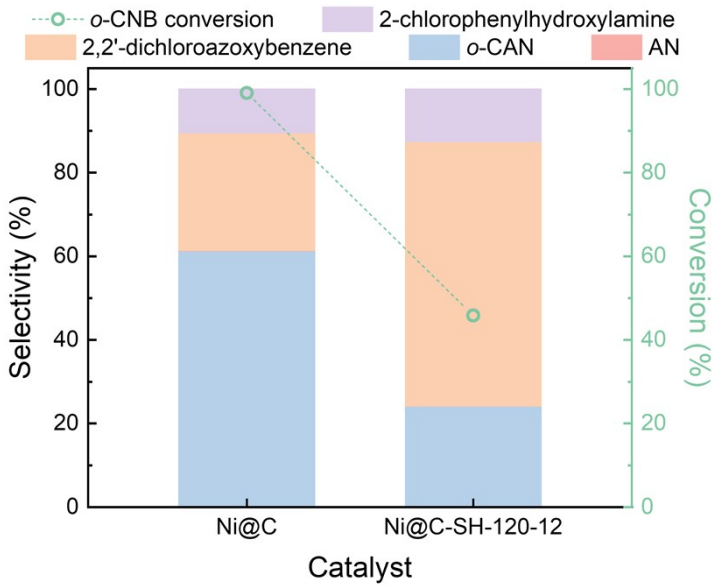

Fig. S12 *o*-CNB conversion and *o*-CAN selectivity over Ni@C and Ni@C-SH-120-12 catalysts. Reaction conditions: 0.5 g *o*-CNB, 0.1 g catalyst, 10.0 g EtOH, 2 MPa H_2, 40 °C, 2 h.

The unmodified catalyst exhibited a 0.2% selectivity for aniline. After thiolate modification, the formation of aniline was completely suppressed, albeit with a moderate decline in hydrogenation activity.

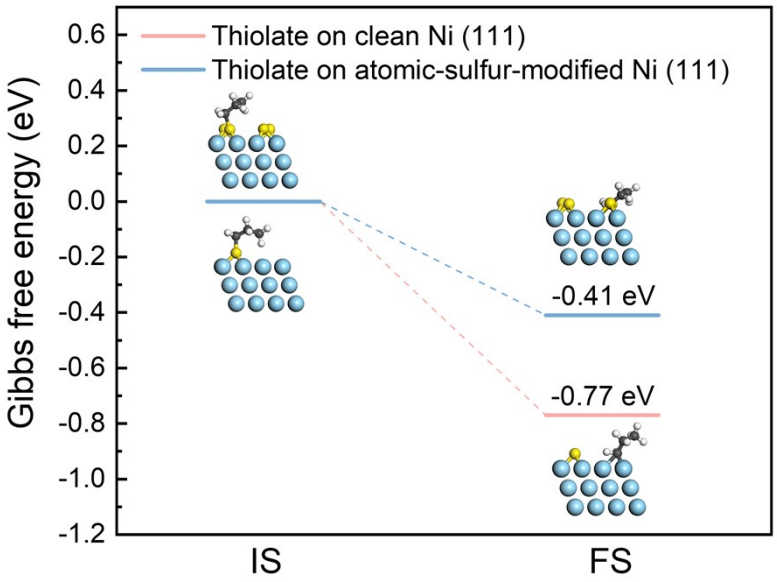

Fig. S13 Gibbs free energy profiles for the C–S bond cleavage of propanethiolate on clean Ni (111) and atomic-sulfur-modified Ni (111).

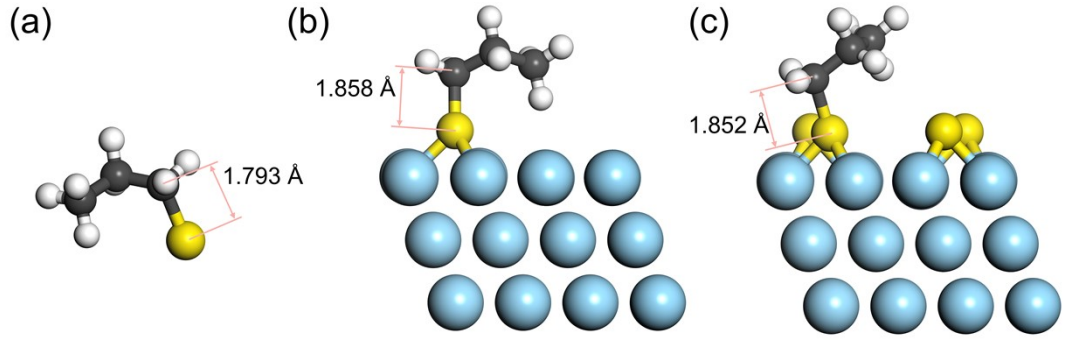

Fig. S14 Calculated C–S bond lengths of propanethiolate ($CH_3CH_2CH_2S$–) under different environments: in vacuum (isolated thiolate), on clean Ni (111), and on Ni (111) with pre-adsorbed atomic sulfur.

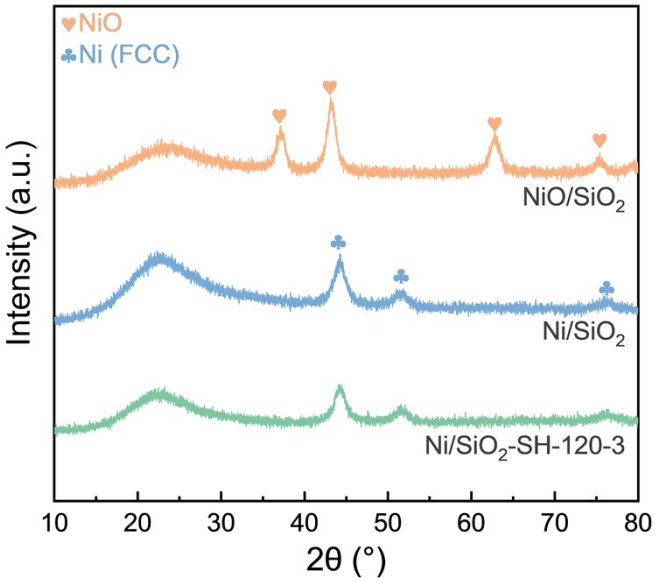

Fig. S15 XRD patterns of NiO/SiO_2, Ni/SiO_2, and Ni/SiO_2-SH-120-3.

The as-prepared NiO/SiO_2 precursor exhibits characteristic diffraction peaks corresponding to the NiO phase. After reduction at 500 °C in H_2, these peaks completely disappear and are replaced by reflections of metallic Ni, confirming the complete conversion to Ni/SiO_2. Notably, subsequent thiolate modification at 120 °C for 3 h does not alter the metallic Ni phase; the XRD pattern of Ni/SiO_2-SH-120-3 shows only the Ni phase with no detectable nickel sulfide or other phases, indicating that the modification remains confined to the surface.

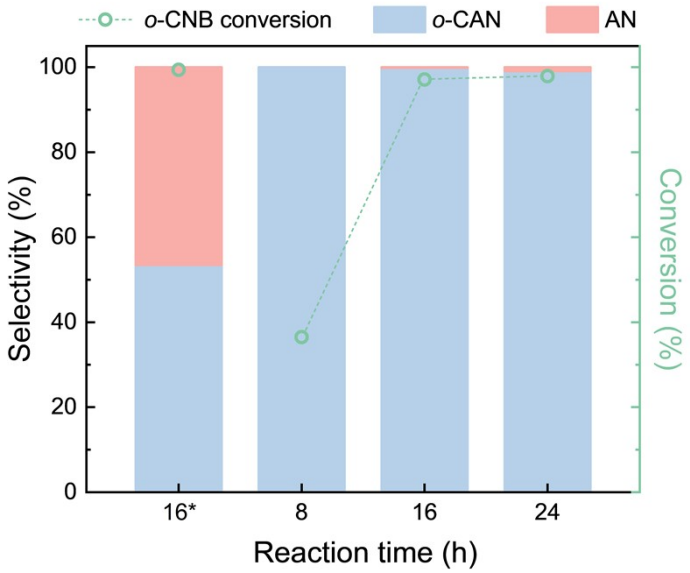

Fig. S16 Catalytic performance of Ni/SiO_2-SH-120-3 in the hydrogenation of *o*-CNB. Reaction conditions: 0.5 g *o*-CNB, 10.0 g EtOH, 2 MPa H_2, 100 °C.
*: The Ni/SiO_2 catalyst.

The unmodified Ni/SiO_2 catalyst exhibited high activity but poor selectivity: after 16 h, *o*-CNB conversion reached 99.4%, yet the selectivity toward *o*-CAN was only 53.5%, with aniline formation accounting for 46.5%. In contrast, the thiolate-modified Ni/SiO_2-SH-120-3 catalyst achieved exceptional selectivity while maintaining good activity. At 8 h, the conversion was 36.5% with an *o*-CAN selectivity of 99.8% (aniline < 0.2%). Prolonging the reaction to 16 h gave 97.1% conversion and 99.8% *o*-CAN selectivity. Even after 24 h, the aniline selectivity remained as low as 0.93%, indicating the remarkable durability of the thiolate adlayer.

It is worth noting that the slightly lower initial activity of Ni/SiO_2-SH-120-3 compared to its carbon-supported counterpart can be attributed to its lower nickel loading (17 wt%) and the mass loss upon reduction of NiO to Ni. Consequently, the absolute amount of Ni sites participating in the reaction is considerably smaller than that in Ni@C. Nevertheless, the high selectivity toward *o*-CAN is sustained over extended reaction times, underscoring the robustness of the modification strategy.

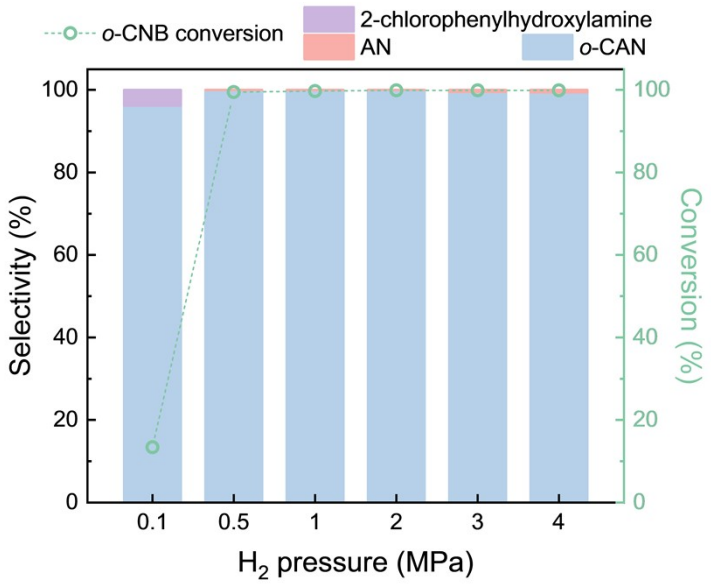

Fig. S17 Effect of H_2 pressure on the hydrogenation of *o*-CNB over the Ni@C-SH-120-12 catalyst. Reaction conditions: 0.5 g *o*-CNB, 0.1 g catalyst, 10.0 g EtOH, 100 °C, 2 h.

At a low pressure of 0.1 MPa, the conversion was limited to 13.4%, and the intermediate 2-chlorophenylhydroxylamine was detected (3.8% selectivity), indicating a stepwise reduction pathway. Remarkably, the selectivity to *o*-CAN remained high (96.2%) even under hydrogen-deficient conditions. Near-quantitative yield of *o*-CAN (99.9%) was achieved at an optimal pressure around 2.0 MPa. Further increasing the pressure to 4.0 MPa sustained complete conversion but led to a slight increase in aniline selectivity (0.6%), suggesting that excessively high surface hydrogen coverage might marginally promote the hydrodechlorination pathway.

Table S4. Performance comparison of representative catalysts for the hydrogenation of chloronitrobenzenes (CNB) to chloroanilines (CAN).

Catalyst	Reaction conditions	Yield after prolonged reaction (time)	Yield after recycling (cycles)	Ref.
Ni@C-SH-120-12 [a]	0.5 g *o*-CNB, 0.1 g catalyst, 10.0 g EtOH, 2 MPa H_2, 100 °C.	>99.9 (16 h)	>99.9% (12 cycles)	This work
NiAl-20	2.1 g *o*-CNB, 150 mg catalyst, 50 mL EtOH, 2 MPa H_2, 50 °C.	90.0 (28 h)	28.9% (3 cycles)	3
PCN-221@Pt@PCN-221(Co)15.1	1 mmol *o*-CNB, 9.98 mg catalyst, 5 mL Methanol, 1 MPa H_2, 80 °C.	97.0 (2 h)	96.0% (10 cycles)	4
Pd/CS_2 [a]	10.0 g *o*-CNB, 0.1 g catalyst, 200 mL EtOH, 1 MPa H_2, 140 °C.	NR	>99.9% (6 cycles)	5
Co/C-500	25.4 mmol *o*-CNB, 0.2 g catalyst, 40 mL EtOH, 3 MPa H_2, 80 °C.	NR	62.0% (6 cycles)	6
Ni/10%TiO_2@OAC-823	15.0 g *m*-CNB, 1.0 g catalyst, 15g EtOH, 2 MPa H_2, 70 °C.	NR	92.8% (6 cycles)	7
$Pt_{2.4}$/SMC	78.8 mg *p*-CNB, 10 mg catalyst, 0.1 MPa H_2.	NR	96.9% (5 cycles)	8
Pd-Au/NPC	0.787 g *p*-CNB, 25 mL Methanol, 1.2 MPa H_2, 100 °C.	NR	51.5% (5 cycles)	9
Pd_1Co_1/NC	0.5 mmol *p*-CNB, 10 mg catalyst, 10.0 mL EtOH, 2 MPa H_2, 100 °C.	99.0 (4 h)	99.0% (7 cycles)	10

[a] Reaction temperature for recycling tests was 80 °C.

NR: Not reported in the original literature.

REFERENCE

1. J. Gu, W. Gong, Q. Zhang, R. Long, J. Ma, X. Wang, J. Li, J. Li, Y. Fan, X. Zheng, S. Qiu, T. Wang and Y. Xiong, *Nat. Commun.*, 2023, 14, 7935.
2. L. Luo, F. Zhu, R. Tian, L. Li, S. Shen, X. Yan and J. Zhang, *ACS Catal.*, 2017, 7, 5420-5430.
3. H. Kan, X. Chou, M. Li, C. Xi, T. Zhou, Z. Xiao and Y. Ding, *Appl. Surf. Sci.*, 2024, 649, 159120.
4. T. Lin, Z. Cao, J. Pei, B. Wang, H. Liu, B. Tu, C. Yang, F. Zheng, W. Chen, Q. Fang, W. Liu, Z. Tang and G. Li, *J. Am. Chem. Soc.*, 2025, 147, 11975-11987.
5. Q. Zhang, K. Li, Y. Xiang, Y. Zhou, Q. Wang, L. Guo, L. Ma, X. Xu, C. Lu, F. Feng, J. Lv, J. Ni and X. Li, *Appl. Catal. A-Gen.*, 2019, 581, 74-81.
6. Q. Wang, Y. Dai, X. Hong, Y. Hong, R. Zhang and X. Yan, *New J. Chem.*, 2024, 48, 7639-7645.
7. L. Huang, Y. Lv, S. Liu, H. Cui, Z. Zhao, H. Zhao, P. Liu, W. Xiong, F. Hao and H. a. Luo, *Ind. Eng. Chem. Res.*, 2020, 59, 1422-1435.
8. J. Li, S. Ding, F. Wang, H. Zhao, J. Kou, M. Akram, M. Xu, W. Gao, C. Liu, H. Yang and Z. Dong, *J. Colloid Interface Sci.*, 2022, 625, 640-650.
9. H. Jing, L. Sun, Q. Xie, Y. Zhai, C. Qi, B. Duan, X. Sun, L. Zhao, M. Zhang and H. Su, *Appl. Catal. A-Gen.*, 2025, 702, 120332.
10. F. Cao, L. Wang, Q. Zhao, H. Liu, W. Ni, Y. Zhang, B. Zhu, Y. Yan, Z. Wang, Z. Li and M. Wu, *ACS Catal.*, 2026.